Polymer Chemistry

ROYAL SOCIETY OF CHEMISTRY

COMMUNICATION

View Article Online
View Journal | View Issue

Cite this: *Polym. Chem.*, 2026, **17**, 897

Received 24th October 2025,
Accepted 10th February 2026

DOI: 10.1039/d5py01009h

rsc.li/polymers

Highly swellable pH-responsive nanogels generated by polymerisation-induced self-assembly

Xueyuan Li,†[a,b] Xiaojing Lu,†[a,b] Jian Tang,[a,b] Francesca Patel-Burrows[a,b] and Lee A. Fielding *[a,b]

The synthesis of pH-responsive nanogels *via* reversible addition–fragmentation chain-transfer (RAFT)-mediated polymerisation-induced self-assembly (PISA) in aqueous media, using poly(potassium 3-sulfopropyl methacrylate)$_{44}$-*block*-poly(2-hydroxypropyl methacrylate$_{1-x\%}$-*stat*-methacrylic acid$_{x\%}$)$_{300}$ (PKSPMA$_{44}$-*b*-P(HPMA$_{1-x\%}$-*stat*-MAA$_{x\%}$)$_{300}$) block copolymers is reported. These nanogels exhibit pronounced and tunable pH-dependent swelling, excellent colloidal stability, and reversibility across multiple pH cycles. These findings advance the design of smart soft materials and establish RAFT-mediated PISA nanogels as promising candidates for pH-triggered delivery systems, biosensing platforms, and adaptive biomaterials.

Introduction

Polymeric nanogels are polymer nanoparticles capable retaining solvent (often referred to as nano-hydrogels in the case of water) and typically exhibit diameters between 20 nm to 200 nm.[1] Nanogels have been broadly investigated and applied in diverse areas, particularly in bioimaging,[2–4] drug-delivery,[5–7] and photosensitisation.[8] Such nanogels can be designed as stimuli-responsive particles responding to pH,[9–17] temperature,[18–22] redox agents,[23,24] light,[25,26] and carbon dioxide.[27–31]

Nanogels incorporating pH-responsive building-blocks provide swelling behaviour through the protonation and deprotonation of ionisable moieties. These nanoparticles can undergo size variation based on cationic or anionic pH-responsive moieties, such as methacrylic acid (MAA),[16,17,32] alginate,[14] 2-(methacryloyloxy) ethyl succinate (MES),[15] 2-(diethylamino)ethyl methacrylate (DEAEMA),[13,33] 2-(dimethylamino) ethyl methacrylate (DMAEMA),[34,35] and chitosan.[9,36,37] Anionic monomers such as MAA and alginate typically cause nanogels to expand at high pH owing to deprotonation, while cationic polymers impart the opposite response due to protonation of *e.g.*, amine groups.

Among the various synthetic routes to fabricate polymer nanoparticles, RAFT-mediated PISA has emerged as a robust and versatile approach. PISA generally employs a solvent-philic stabiliser block and a solvent-phobic core-forming block, allowing direct nanoparticle formation at high solids contents.[38] Recently, pH-responsive PISA-derived nanogels have been reported. For example, in 2024 Du *et al.* reported a series of pH-responsive nanogels synthesised employing poly(potassium 3-sulfopropyl methacrylate) (PKSPMA) as a macromolecular chain-transfer agent (macro-CTA) and stabiliser block, which was chain-extended with poly(benzyl methacrylate-*stat*-methacrylic acid) as the core-forming block.[15] The swelling behaviour of the resulting nanogels was tuned by adjusting the relative composition of MAA and benzyl methacrylate (BzMA) within the core-forming region. A nanogel with a composition of 20 mol% MAA in the core exhibited an increase in diameter from 51 nm at pH 2 to 84 nm at pH 10. The swelling performance of PISA-derived nanogels was improved in subsequent work by employing a different core-forming monomer.[16] In this case, a relatively hydrophobic carboxylic acid-functional monomer, 2-(methacryloyloxy)ethyl succinate (MES), was used as the core-forming block. The resulting nanogels exhibited more pronounced pH responsiveness, swelling from 66 nm at pH 2 to 143 nm at pH 10, or from 150 nm at pH 2 to 280 nm at pH 10, depending on the formulation. For both formulations the resulting nanogels were investigated as the basis of polymer-nanoparticle-based complex coacervate (PNCC) hydrogels, where the degree of swelling of the selected nanogels directly impacted bulk PNCC gel properties.[15,17] Thus, the development of PISA-derived nanogel systems with increased swelling properties is of high importance for ongoing work in

[a]*Department of Materials, School of Natural Sciences, The University of Manchester, Oxford Road, Manchester M13 9PL, UK. E-mail: lee.fielding@manchester.ac.uk*
[b]*Henry Royce Institute, The University of Manchester, Oxford Road, Manchester M13 9PL, UK*
†These authors should be considered as co-first authors.

this area. Importantly, the formation of nanoparticles normally requires either crosslinkers[32,39] or a strongly hydrophobic core-forming block[40,41] to prevent the disassembly.

Herein, a novel PISA-derived nanogel composition is reported based on a poly(2-hydroxypropyl methacrylate-*stat*-methacrylic acid) core-forming block, without the use of any additional crosslinker. It was hypothesised that this *dispersion polymerisation* formulation would facilitate the preparation of more swellable nanogels compared with *emulsion polymerisation* formulations previously reported.[15,16] The resulting nanogels exhibit, to the best of our knowledge, the most pronounced pH-responsive swelling behaviour reported for such systems to date, as judged by dynamic light scattering (DLS) studies. Thus, these nanogels have the potential to serve as a platform to further develop pH-responsive soft material systems.

Results and discussion

The successful RAFT solution polymerisation of KSPMA, targeting a degree of polymerisation (DP) of 50 (Fig. 1a), was confirmed by ^{1}H NMR and aqueous gel permeation chromatography (GPC) measurements (Fig. S1, SI). Kinetic studies were conducted, with monomer conversion increasing throughout the polymerisation (Fig. S1b) and $\ln([M]_n/[M]_0)$ *versus* reaction time (Fig. S1c) exhibiting a linear relationship (R^2 = 0.98), indicating pseudo first-order kinetics. Aqueous GPC (Fig. S1a) indicated M_n = 12 500 g mol^{-1} and a narrow molar mass distribution (M_w/M_n = 1.10), suggesting good RAFT control during the synthesis.

The preparation of PKSPMA$_{44}$-*b*-P(HPMA$_{1-x\%}$-*stat*-MAA$_{x\%}$)$_{300}$ nanoparticles with varying HPMA and MAA compositions was achieved *via* RAFT-mediated PISA. Unlike a previous study from our group which investigated BzMA and MAA as binary core-forming monomers in primarily an emulsion polymerisation formulation,[15] the use of more hydrophilic HPMA in place of BzMA presumably facilitates this to fully be a dispersion polymerisation reaction.[46,47] This difference inevitably changes the assembly of the growing block copolymer and resulting nanoparticles in terms of the chain aggregation number and degree of solvation; factors which were hypothesised to result in differing degrees of nanogel swellability. In addition, increased core solvation and the greater hydrophilicity of HPMA (compared to BzMA) during the polymerisation was hypothesised to promote increased diffusion of MAA into the core-forming region of the nascent nanoparticles throughout the polymerisation, resulting in more random statistical blocks, and potentially increased degrees of swelling.

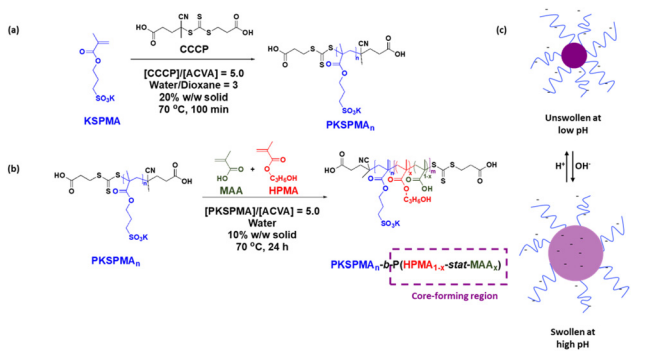

Fig. 1 (a) Synthesis of poly(potassium 3-sulfopropyl methacrylate) (PSKPMA) *via* RAFT-mediated solution polymerisation. (b) Chain extension of PKSPMA with methacrylic acid (MAA) and hydroxypropyl methacrylate (HPMA) *via* RAFT-mediated dispersion polymerisation. (c) Schematic illustration of pH-responsive behaviour of the prepared nanoparticles.

A series of PKSPMA-*b*-P(HPMA$_{1-x\%}$-*stat*-MAA$_{x\%}$) nanoparticles, denoted as S-(H$_{1-x\%}$-A$_{x\%}$), were successfully prepared, achieving high monomer conversions without the need for pH adjustment. Nanoparticle formulations with varying MAA compositions exhibited conversions exceeding 99% in all cases, as determined by ^{1}H NMR analysis (Fig. S2, SI), indicating good compatibility between MAA and HPMA during the copolymerisation process.

Nanoparticles were successfully formed when the content of MAA in the 2nd block was between 0 and 30 mol%. DLS confirmed the formation of well-dispersed nanoparticles with hydrodynamic diameters ranging from approximately 120 to 200 nm at pH 4, and zeta-potentials of approximately −50 mV, indicating good colloidal stability due to electrostatic repulsion (Fig. 2). In addition, the morphology of a representative sample, S$_{44}$-(H$_{75\%}$-A$_{25\%}$)$_{300}$, was analysed by TEM at pH4 (Fig. S3, SI), which confirmed the formation of relatively spherical nanoparticles with mean diameters of approximately 160 nm, in good agreement with the DLS data. Above the threshold of 30 mol% MAA, the copolymer dispersions were visually translucent, potentially because the copolymers were unable to fully self-assemble into nanoparticles. This is attributed to the reduced hydrophobicity of the 'core-forming' block at higher MAA contents disfavouring self-assembly. In addition, it should be noted that no additional di-vinyl crosslinking comonomer was used in these formulations. The intention of this was to achieve the highest possible degree of swelling, as chemical crosslinking would restrict polymer chain mobility, reduce the hydrophilicity of the core, and consequently limit volume expansion upon pH variation. Moreover, previous reports on analogous MES- and BzMA-based systems demonstrated that such crosslinking was unnecessary for maintaining particle integrity.[15–17]

The pH-responsive behaviour of these nanoparticles was tested between pH 4 and 10 to investigate their swelling characteristics (Fig. 1c). As expected, nanoparticles without MAA exhibited no significant change in hydrodynamic diameter upon titration (Fig. 2a), confirming the pH-insensitive nature of the PHPMA core-forming block. In addition, the zeta potential of the nanoparticles remained consistently anionic, as expected for PKSPMA-stabilised particles.[16,17,40,42] In contrast, all MAA-containing nanoparticles displayed similar behaviour whereby the particle diameter increased on increasing the pH, reaching a maximum at approximately pH 8, and then slightly decreasing at higher pH values (Fig. 2). The

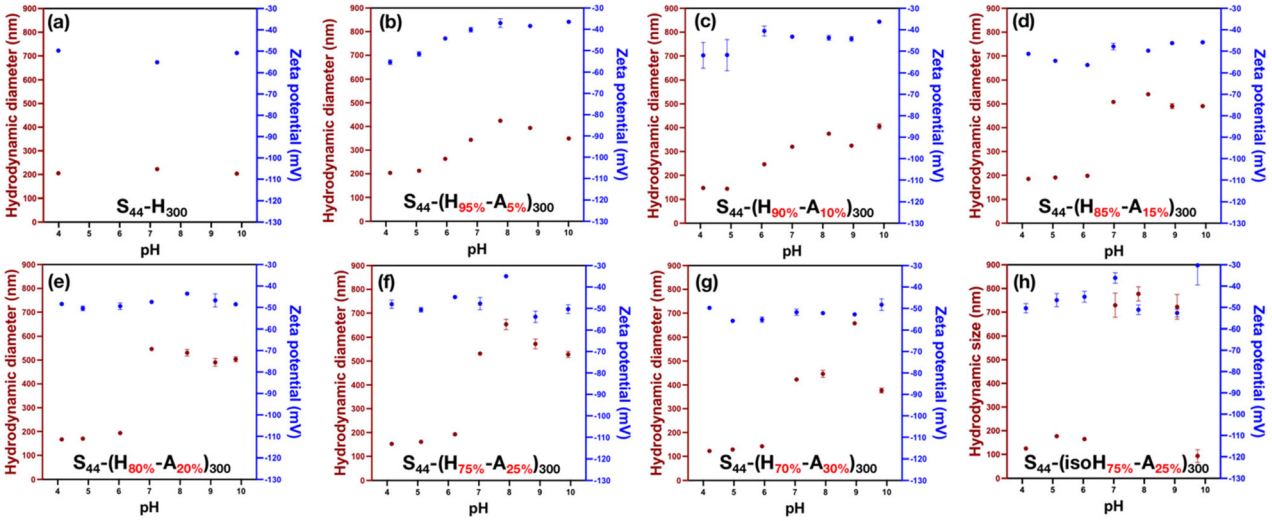

Fig. 2 Hydrodynamic diameter and zeta potential of PKSPMA$_{44}$-P(HPMA$_{1-x\%}$-MAA$_{x\%}$)$_{300}$ plotted against pH. Samples were prepared at 25 °C and 0.10% w/w. (a) S$_{44}$-H$_{300}$ (b) S$_{44}$-(H$_{95\%}$-A$_{5\%}$)$_{300}$ (c) S$_{44}$-(H$_{90\%}$-A$_{10\%}$)$_{300}$ (d) S$_{44}$-(H$_{85\%}$-A$_{15\%}$)$_{300}$ (e) S$_{44}$-(H$_{80\%}$-A$_{20\%}$)$_{300}$ (f) S$_{44}$-(H$_{75\%}$-A$_{25\%}$)$_{300}$ (g) S$_{44}$-(H$_{70\%}$-A$_{30\%}$)$_{300}$ (h) S$_{44}$-(isoH$_{75\%}$-A$_{25\%}$)$_{300}$.

initial increase in particle diameter is attributed to the deprotonation of carboxylic acid groups in the core of the nanoparticles, leading to enhanced intermolecular electrostatic repulsion, thus swelling of the nanoparticle cores. The zeta-potential of these MAA-containing samples remained highly negative (<−30 mV) across the entire pH range, due to the strongly anionic PKSPMA stabiliser.

A slight reduction in the zeta-potential magnitude was observed upon increasing pH, which can be attributed to the swelling of the nanoparticle core, leading to decreased charge density near the particle surface. Upon further addition of potassium hydroxide during titration, the ionic strength of the colloidal system increased, resulting in charge shielding of the deprotonated carboxylic acid groups and a corresponding slight decrease in particle sized observed by DLS measurements.

The swelling behaviour of these nanoparticles is summarised in Table S1 (SI). Interestingly, D_h values at pH 4 decreased moderately with increasing MAA content, falling from 205 nm in the absence of MAA to 123 nm with 30% MAA. This observation may be attributed to the hypothesis that PMAA behaves as a core-compacting component at low pH due to the formation of hydrogen bonds. Conversely, an alternative explanation is that nanoparticles with higher PMAA contents may possess lower aggregation numbers (*i.e.*, fewer chains per particle), possibly due to increased ease of chain exchange, resulting in a larger number of more solvated or loosely associated micelles. These possibilities cannot be confirmed from the current data and will be the subject of future investigation using *e.g.*, small-angle X-ray scattering.

The maximum swelling ratio increased from 1.1 to 2.1 with the inclusion of just 5 mol% MAA in the core forming block and increased further to 4.3 with 25 mol% MAA. This trend is somewhat expected and is attributable to greater amount of core ionisation with increased MAA content, where the increased electrostatic repulsion between deprotonated chains promotes greater water uptake and thus more pronounced swelling. Nevertheless, no evidence of particle disassociation was observed by DLS or by visible inspection of the resulting dispersions on increasing the pH for samples up to 25 mol% MAA. However, the reduction in swelling degree for S$_{44}$-(H$_{70\%}$-A$_{30\%}$)$_{300}$ may indicate some particle dissociation occurs with high MAA contents in the absence of additional crosslinker, as the core-forming block requires some degree of hydrophobicity to maintain structural integrity. Unfortunately, these observations could not be supported by TEM analysis as these nanogels could not be imaged in the swollen state and will be the subject of additional investigations in the future.

Reversibility of the pH-induced swelling was examined for S$_{44}$-(H$_{75\%}$-A$_{25\%}$)$_{300}$ nanoparticles by adjusting the pH between 4 and 8 repeatedly (Fig. 3). As expected, the nanogels continued to

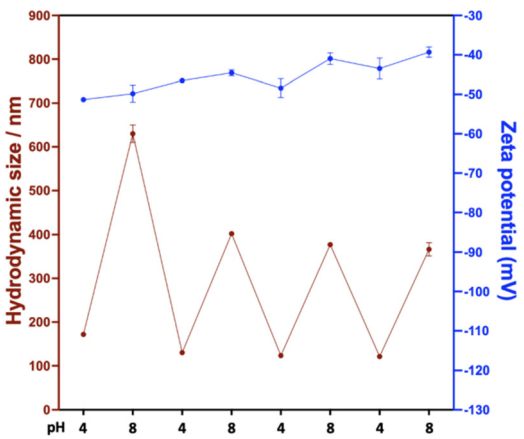

Fig. 3 Variation in particle size with pH cycling between 4 and 8 for S$_{44}$-(H$_{75\%}$-A$_{25\%}$)$_{300}$ dispersions at 25 °C containing 1 mM KCl.

swell/de-swell over at least 4 pH cycles. Interestingly, the swollen diameter measured during the 1st cycle was significantly larger than for subsequent cycles, and the diameters at both pH 4 and pH 8 gradually decreased over successive pH titration cycles. These observations can primarily be attributed to the build-up of ionic strength during these experiments, which screens the charges of the deprotonated carboxylic acid groups within the core and consequently reduces the influx of water into the core of the nanoparticles and thus the degree of swelling. The first cycle shows the most pronounced decrease in diameter because it experiences the largest change in ionic strength. In addition, some segment rearrangement may occur in the absence of cross-linkers. Deprotonated carboxylic acid groups electrostatically repel each other after deprotonation, whereas they likely form hydrogen-bonds in the pristine nanoparticles. This correlates well with the observed decrease in the absolute zeta-potential values recorded during each pH cycle. In addition, the initial dramatic change could also potentially be due to loss of copolymer chains from individual particles in the swollen state. Nevertheless, it is apparent that the majority of the nanogels remain intact, close to their initial unswollen diameter, and continue to display reversible behaviour.

The nanogels discussed thus far employed HPMA monomer which is supplied as a mixture of isomers, with the formulation containing 25 mol% MAA exhibiting the highest degree of swelling. To investigate whether the use of a single HPMA isomer influences nanogel formation and swelling behaviour, 2-hydroxyisopropyl methacrylate (isoHPMA) was used in place of the isomeric mixture for a formulation containing 25 mol% MAA. This isoHPMA-based nanogel displayed a comparable hydrodynamic diameter in the unswollen state but exhibited a markedly greater swelling ratio of 6.2, indicating that the isomeric composition of HPMA plays a role in controlling self-assembly and the resulting nanogel properties. It is somewhat surprising given the very similar structures of HPMA and isoHPMA that such a subtle isomeric difference leads to a markedly increased swelling ratio. This behaviour may arise from increased steric hindrance of the hydroxyl group in isoHPMA, which favours hydrogen bonding between the pendant hydroxyl groups and surrounding water molecules rather than another pendent group. As a result, the isoHPMA-based nanogels are able to take up more water upon deprotonation at higher pH, leading to their enhanced swelling.

PHPMA-based PISA-derived nano-objects are well known to display thermoresponsive behaviour, often undergoing sphere–worm–vesicle transitions, as reported for PGMA–PHPMA systems.[21,43–45] Such effects are typically observed for formulations prepared using mixed or isoHPMA monomers due to hydrogen bonding between water molecules and the isopropanol hydroxyl groups. Thus, the temperature responsiveness of the S_{44}-$(isoH_{75\%}$-$A_{25\%})_{300}$ nanogels was investigated between 1 °C and 45 °C using heating/cooling cycles (Fig. S4, SI). Interestingly, no significant thermal response was observed in the swollen or unswollen state, despite the presence of the isopropyl functionality. This absence of temperature sensitivity is potentially surprising, as one might expect dissociation of the nanoparticles to unimers on cooling. However, the presence of the carboxylic acid functionality of MAA likely contributes to maintaining structural integrity, preventing temperature-induced disassembly. It appears that the hydrogen bonding occurring predominantly between hydroxyl and carboxylic acid groups within the core-forming region, rather than with water molecules, results in a structure that is relatively insensitive to temperature changes.

Conclusions

In summary, a series of well-defined PKSPMA$_{44}$-*b*-P(HPMA$_{1-x\%}$-*stat*-MAA$_{x\%}$)$_{300}$ amphiphilic block copolymer nanoparticles were successfully synthesised *via* RAFT-mediated aqueous dispersion polymerisation. The polymerisation of KSPMA proceeded in a controlled manner, as confirmed by ^{1}H NMR and aqueous GPC studies. Subsequent chain extension with HPMA and MAA produced colloidally stable nanoparticles exhibiting tuneable compositions and pronounced pH-responsive behaviour, as demonstrated by DLS analysis.

Self-assembly occurred through hydrophobic interactions when the MAA content of the 2nd block was 30 mol% or below, without requiring additional cross-linking comonomer. The incorporation of MAA imparted pH-dependent swelling behaviour, with particle diameter increasing upon deprotonation of carboxylic acid groups and reversibly decreasing at low pH. The nanogels also showed reversible size transitions during cyclic pH variation between 4 and 8, demonstrating good structural stability and reproducibility.

Surprisingly, no significant thermal-response was observed for these hydroxypropyl methacrylate-based systems, even when using hydroxyisopropyl methacrylate. This lack of temperature sensitivity is attributed to strong hydrogen bonding between hydroxyl and carboxylic acid groups within the core, forming a compact and thermally stable structure.

Overall, this study demonstrates the synthesis and characterisation of highly swellable, pH-responsive nanogels *via* a RAFT-mediated PISA process. To the best of our knowledge, these nanogels exhibit the most pronounced swelling behaviour of this class of nanogels reported to date. It is worth noting that a reviewer raised the point that the absence of crosslinker may be not that advantageous for certain applications. We acknowledge that the absence of covalent crosslinking may limit mechanical robustness in some contexts; however, the exceptional swelling enabled by this non-crosslinked design provides distinct advantages for applications that rely on pronounced pH-responsive behaviour, offering valuable potential for future applications such as in pH-sensitive drug delivery and other stimuli-responsive soft material systems.

Author contributions

Xueyuan Li: writing – review & editing, writing – original draft, validation, methodology, investigation, formal analysis, data

curation, conceptualisation. Xiaojing Lu: writing – original draft, methodology, investigation, formal analysis. Jian Tang: investigation. Francesca Patel-Burrows: investigation. Lee A. Fielding: writing – review & editing, supervision, resources, project administration, methodology, funding acquisition, formal analysis, data curation, conceptualisation.

Conflicts of interest

There are no conflicts to declare.

Data availability

The data supporting this article have been included as part of the supplementary information (SI). Supplementary information: Materials and methods, GPC data, ^{1}H NMR spectra, TEM images, particle diameter *versus* temperature, and summary table of swelling behaviour of reported copolymers. See DOI: https://doi.org/10.1039/d5py01009h.

Acknowledgements

The University of Manchester Electron Microscopy Centre is acknowledged for access to electron microscopy facilities. This work was supported by the Henry Royce Institute for Advanced Materials, funded through EPSRC grants EP/R00661X/1, EP/S019367/1, EP/P025021/1, and EP/P025498/1 and the Sustainable Materials Innovation Hub, funded through the European Regional Development Fund OC15R19P.

References

1 K. S. Soni, S. S. Desale and T. K. Bronich, *J. Controlled Release*, 2016, **240**, 109–126.
2 X. Wang, D. Niu, P. Li, Q. Wu, X. Bo, B. Liu, S. Bao, T. Su, H. Xu and Q. Wang, *ACS Nano*, 2015, **9**, 5646–5656.
3 V. M. Vijayan, A. E. Beeran, S. J. Shenoy, J. Muthu and V. Thomas, *ACS Appl. Bio Mater.*, 2019, **2**, 757–768.
4 W. Zhang, B. Du, M. Gao and C.-H. Tung, *ACS Nano*, 2021, **15**, 16442–16451.
5 F. Meng, Z. Zhong and J. Feijen, *Biomacromolecules*, 2009, **10**, 197–209.
6 Y. Li, Q. N. Bui, L. T. M. Duy, H. Y. Yang and D. S. Lee, *Biomacromolecules*, 2018, **19**, 2062–2070.
7 D. Chen, H. Yu, K. Sun, W. Liu and H. Wang, *Drug Delivery*, 2014, **21**, 258–264.
8 H. He, A.-L. Nieminen and P. Xu, *Biomater. Sci.*, 2019, **7**, 5143–5149.
9 T. Zhou, C. Xiao, J. Fan, S. Chen, J. Shen, W. Wu and S. Zhou, *Acta Biomater.*, 2013, **9**, 4546–4557.
10 J. R. Lovett, N. J. Warren, L. P. D. Ratcliffe, M. K. Kocik and S. P. Armes, *Angew. Chem., Int. Ed.*, 2015, **54**, 1279–1283.
11 N. J. W. Penfold, J. R. Lovett, N. J. Warren, P. Verstraete, J. Smets and S. P. Armes, *Polym. Chem.*, 2016, **7**, 79–88.
12 S. L. Canning, T. J. Neal and S. P. Armes, *Macromolecules*, 2017, **50**, 6108–6116.
13 A. Pikabea, E. Villar-Álvarez, J. Forcada and P. Taboada, *J. Mol. Liq.*, 2018, **266**, 321–329.
14 G. Geyik, E. Güncüm and N. Işıklan, *Int. J. Biol. Macromol.*, 2023, **250**, 126242.
15 R. Du and L. A. Fielding, *Soft Matter*, 2023, **19**, 2074–2081.
16 R. Du and L. A. Fielding, *Macromolecules*, 2024, **57**, 3496–3501.
17 R. Du, X. Li and L. A. Fielding, *Langmuir*, 2024, **40**, 20648–20656.
18 N. J. Warren and S. P. Armes, *J. Am. Chem. Soc.*, 2014, **136**, 10174–10185.
19 L. A. Fielding, J. A. Lane, M. J. Derry, O. O. Mykhaylyk and S. P. Armes, *J. Am. Chem. Soc.*, 2014, **136**, 5790–5798.
20 Q.-T. Pham, Z.-H. Yao, Y.-T. Chang, F.-M. Wang and C.-S. Chern, *J. Taiwan Inst. Chem. Eng.*, 2018, **93**, 63–69.
21 Q. Yue, Z. Luo, X. Li and L. A. Fielding, *Soft Matter*, 2023, **19**, 6513–6524.
22 T. Nakagawa, S. Ishino, D. Inamori, H. Masai and J. Terao, *ACS Macro Lett.*, 2023, **12**, 751–758.
23 Y. Zhou, Z. Wang, Y. Wang, L. Li, N. Zhou, Y. Cai, Z. Zhang and X. Zhu, *Polym. Chem.*, 2020, **11**, 5619–5629.
24 J. Sarkar, K. B. J. Chan and A. Goto, *Polym. Chem.*, 2021, **12**, 1060–1067.
25 D. Wang and X. Wang, *Prog. Polym. Sci.*, 2013, **38**, 271–301.
26 M. Huo, Q. Ye, H. Che, X. Wang, Y. Wei and J. Yuan, *Macromolecules*, 2017, **50**, 1126–1133.
27 A. Darabi, P. G. Jessop and M. F. Cunningham, *Chem. Soc. Rev.*, 2016, **45**, 4391–4436.
28 M. Zeng, M. Huo, Y. Feng and J. Yuan, *Macromol. Rapid Commun.*, 2018, **39**, 1800291.
29 L. Yu, Y. Zhang, X. Dai, Q. Xu, L. Zhang and J. Tan, *Chem. Commun.*, 2019, **55**, 11920–11923.
30 D. Zhou, R. P. Kuchel, S. Dong, F. P. Lucien, S. Perrier and P. B. Zetterlund, *Macromol. Rapid Commun.*, 2019, **40**, 1800335.
31 L. Qiu, H. Zhang, B. Wang, Y. Zhan, C. Xing and C.-Y. Pan, *ACS Appl. Mater. Interfaces*, 2020, **12**, 1348–1358.
32 T. Sun, J. Zhang, Y. Cen, S. Zhong, B. Liu, Y. Yang, B. Yu, X. Sun, B. Peng, D.-S. Bin, J. Wang and Y. Ning, *J. Colloid Interface Sci.*, 2026, **703**, 139150.
33 M. K. Notabi, E. C. Arnspang, N. A. Peppas and M. Ø. Andersen, *J. Drug Delivery Sci. Technol.*, 2023, **86**, 104510.
34 A. Roointan, J. Farzanfar, S. Mohammadi-Samani, A. Behzad-Behbahani and F. Farjadian, *Int. J. Pharm.*, 2018, **552**, 301–311.
35 X. Du, Y. Peng, C. Zhao and J. Xing, *Colloids Surf., B*, 2022, **217**, 112611.
36 W. Wu, J. Shen, P. Banerjee and S. Zhou, *Biomaterials*, 2010, **31**, 8371–8381.
37 M. Arteche Pujana, L. Pérez-Álvarez, L. C. Cesteros Iturbe and I. Katime, *Eur. Polym. J.*, 2014, **61**, 215–225.

38 S. P. Armes, S. Perrier and P. B. Zetterlund, *Polym. Chem.*, 2021, **12**, 8–11.
39 Y. Dong, J. Chi, Z. Ren, B. Xiong, Z. Liu, W. Zhang, L. Wang, S. Fujii, S. P. Armes and Y. Ning, *Angew. Chem., Int. Ed.*, 2023, **62**, e202300031.
40 S.-P. Wen, J. G. Saunders and L. A. Fielding, *Polym. Chem.*, 2020, **11**, 3416–3426.
41 W. Chen, P. Liu, X. Sun, B. Xiong, H. Cui, Z. Zhao and Y. Ning, *Angew. Chem., Int. Ed.*, 2024, **63**, e202410908.
42 I. Chaduc, M. Lansalot, F. D'Agosto and B. Charleux, *Macromolecules*, 2012, **45**, 1241–1247.
43 A. Blanazs, R. Verber, O. O. Mykhaylyk, A. J. Ryan, J. Z. Heath, C. W. I. Douglas and S. P. Armes, *J. Am. Chem. Soc.*, 2012, **134**, 9741–9748.
44 N. J. Warren, M. J. Derry, O. O. Mykhaylyk, J. R. Lovett, L. P. D. Ratcliffe, V. Ladmiral, A. Blanazs, L. A. Fielding and S. P. Armes, *Macromolecules*, 2018, **51**, 8357–8371.
45 X. Li, Z. Luo and L. A. Fielding, *Macromolecules*, 2025, **58**, 5995–6004.
46 S. M. North and S. P. Armes, *Polym. Chem.*, 2020, **11**, 2147–2156.
47 L. A. Fielding, C. T. Hendley IV, E. Asenath-Smith, L. Estroff and S. P. Armes, *Polym. Chem.*, 2019, **10**, 5131–5141.